

UC San Diego

UC San Diego Previously Published Works

Title

Task fMRI paradigms may capture more behaviorally relevant information than resting-state functional connectivity

Permalink

<https://escholarship.org/uc/item/39p7g4x2>

Authors

Zhao, Weiqi

Makowski, Carolina

Hagler, Donald J

et al.

Publication Date

2023-04-01

DOI

10.1016/j.neuroimage.2023.119946

Peer reviewed

1 Task fMRI paradigms may capture more behaviorally relevant information than resting-state

2 functional connectivity

3
4 Weiqi Zhao^{1,3}, Carolina Makowski^{2,3}, Donald J. Hagler³, Hugh P. Garavan⁴, Wesley K.
5 Thompson⁵, Deanna J. Greene^{1,3}, Terry L. Jernigan^{1,2,3,6,9} & Anders M. Dale^{2,7,8,9} *

6

7 1. Department of Cognitive Science, University of California, San Diego, 9500 Gilman
8 Drive, La Jolla, CA 92093, USA

9 2. Department of Radiology, University of California, San Diego School of Medicine, 9500
10 Gilman Drive, La Jolla, CA 92037, USA

11 3. University of California, San Diego, 9500 Gilman Drive, La Jolla, CA 92161, USA

12 4. University of Vermont, Burlington, Vermont, 05405, USA

13 5. Laureate Institute for Brain Research, Tulsa, OK, 74136, USA

14 6. Center for Human Development, University of California, San Diego, 9500 Gilman
15 Drive, La Jolla, CA 92161, USA

16 7. Center for Multimodal Imaging and Genetics, University of California, San Diego School
17 of Medicine, 9444 Medical Center Dr, La Jolla, CA 92037, USA

18 8. Department of Neuroscience, University of California, San Diego School of Medicine,
19 9500 Gilman Drive, La Jolla, CA 92037, USA

20 9. Department of Psychiatry, University of California, San Diego School of Medicine, 9500
21 Gilman Drive, La Jolla, CA 92037, USA

22 * Correspondence to: amdale@health.ucsd.edu

23

24 Word count (omitting abstract, references): 8571

25 Reference: 62. Figures: 4. Tables: 2.

26 **Highlights:**

27 ● Functional connectivity (FC) patterns derived from fMRI tasks outperform resting-state
28 FC at predicting individual differences in a measure of cognitive task performance and a
29 task-derived behavioral inhibition measure.

30 ● The improvement in behavioral prediction afforded by fMRI tasks over resting-state is
31 largely associated with the FC of the task model fit.

32 ● FC of the task model fit and task design model parameters contain shared and unique
33 behavioral prediction power.

34

Abstract

35
36 Characterizing the optimal fMRI paradigms for detecting behaviorally relevant functional
37 connectivity (FC) patterns is a critical step to furthering our knowledge of the neural basis of
38 behavior. Previous studies suggested that FC patterns derived from task fMRI paradigms, which
39 we refer to as task-based FC, are better correlated with individual differences in behavior than
40 resting-state FC, but the consistency and generalizability of this advantage across task conditions
41 was not fully explored. Using data from resting-state fMRI and three fMRI tasks from the
42 Adolescent Brain Cognitive Development Study[®] (ABCD), we tested whether the observed
43 improvement in behavioral prediction power of task-based FC can be attributed to changes in
44 brain activity induced by the task design. We decomposed the task fMRI time course of each
45 task into the task model fit (the fitted time course of the task condition regressors from the single-
46 subject general linear model) and the task model residuals, calculated their respective FC, and
47 compared the behavioral prediction performance of these FC estimates to resting-state FC and
48 the original task-based FC. The FC of the task model fit was better than the FC of the task model
49 residual and resting-state FC at predicting a measure of general cognitive ability or two measures
50 of performance on the fMRI tasks. The superior behavioral prediction performance of the FC of
51 the task model fit was content-specific insofar as it was only observed for fMRI tasks that probed
52 similar cognitive constructs to the predicted behavior of interest. To our surprise, the task model
53 parameters, the beta estimates of the task condition regressors, were equally if not more
54 predictive of behavioral differences than all FC measures. These results showed that the observed
55 improvement of behavioral prediction afforded by task-based FC was largely driven by the FC
56 patterns associated with the task design. Together with previous studies, our findings highlighted

57 the importance of task design in eliciting behaviorally meaningful brain activation and FC
58 patterns.

59

60 **Keywords:** behavioral differences, predictive modeling, functional connectivity, cognitive
61 development, behavioral inhibition

62

1. Introduction

63

64 An important aim of cognitive neuroscience is to understand how individual differences
65 in behavioral attributes are associated with brain structure and function. With the availability of
66 large neuroimaging datasets, recent work has pivoted towards building models that predict
67 current or future behavior based on neuroimaging measures (Gabrieli, Ghosh, Whitfield-Gabrieli,
68 2015; Varoquaux & Poldrack, 2019; Finn & Rosenberg, 2021). Such predictive modeling
69 approaches allow us to estimate better the degree to which behavioral differences are associated
70 with individual differences in brain structure or function.

71 Trait differences can be predicted by individual differences in functional connectivity
72 (FC), which measures the correlation of the BOLD response across regions of interests (ROIs)
73 across brain regions by calculating the pairwise correlations of fMRI time series (Speer et al.,
74 2021; Zhang et al., 2021). FC patterns are unique to an individual (Finn et al., 2015; Gratton et
75 al., 2018), relatively stable across different mental states (Cole et al., 2014; Finn et al., 2015;
76 Gratton et al., 2018), and sensitive to phenotypic differences including age (Dosenbach et al.,
77 2010; Nielsen et al., 2019), cognitive abilities (Sripada et al., 2019, Moutoussis et al., 2021,
78 Zhang et al., 2021; Chen et al., 2022), and mental health outcomes (Challis et al., 2015, Kim et
79 al., 2016, Thomas et al., 2020; Chen et al., 2022).

80 FC is often estimated during resting-state fMRI acquisitions where participants are not
81 engaged in a particular task but are simply instructed to either close their eyes or fixate on a
82 crosshair and stay still. While resting-state fMRI has become the most common paradigm used
83 for correlating FC patterns with behavioral traits or conditions, there is increasing evidence that
84 rest may not always be the optimal condition to elicit FC patterns that are most relevant to

85 differences in behavioral phenotypes in a particular domain (Rosenberg et al., 2016; Greene et
86 al., 2018; Jiang et al., 2019; Finn, 2021). Naturalistic tasks or traditional fMRI tasks may have
87 more utility for the prediction of trait or state differences as they can elicit cognitive states that
88 are directly relevant to the behavioral domain of interest (Finn et al., 2017).

89 Direct comparisons between resting-state FC (rsFC) and task-fMRI FC suggest that the
90 latter is better at predicting both fMRI attention task performance and trait measures of attention
91 function (Rosenberg et al., 2016), measures of general cognitive ability (Greene et al., 2018;
92 Elliot et al., 2019) and reading comprehension (Jiang et al., 2020). A similar advantage has been
93 shown for more passive task fMRI with naturalistic paradigms such that FC during movie-
94 watching paradigms outperformed rsFC in predicting individual differences in cognitive task
95 performance and emotional health (Finn & Bandettini, 2021).

96 Why might FC patterns derived from task and naturalistic paradigms be more predictive
97 of trait differences than FC patterns derived from rest? Finn and colleagues (Finn et al., 2017;
98 Finn & Bandettini, 2021) proposed that task fMRI and naturalistic paradigms are better
99 candidates than resting-state for the study of behavioral differences because tasks are tailored to
100 engage a particular behavioral domain. Like a cardiac stress test where the heart's ability to
101 respond to external stress is measured by inducing stress in a controlled environment, fMRI tasks
102 and naturalistic paradigms can introduce cognitive and emotional challenges to simulate brain
103 activity. It follows that an fMRI paradigm that engages the behavioral or cognitive processes
104 involved in the behavioral phenotype of interest is likely to amplify brain-behavior relationships
105 (Greene et al., 2020; Greene et al., 2018). In other words, the greater behavioral relevance of the
106 FC derived from task fMRI paradigms may be attributable to the task effects.

107 Previous studies examining FC during fMRI tasks differ in whether they retain the task
108 effects in the fMRI time course for FC estimation. With an explicit task design, the observed
109 time course during a fMRI task can be decomposed into the part that is explained by the task,
110 estimated by the task model fit, and the residual. If the task effect is retained (Vanderwal et al.,
111 2017; Greene et al., 2018; Gao et al., 2019), the FC estimates, which we label the *task-based FC*,
112 capture the FC of the original and complete task fMRI time series (See Table 1 for a description
113 of all fMRI measures used in this study). While numerous studies have reported the advantage of
114 task-based FC at predicting behavioral traits (Greene et al., 2018; Elliot et al., 2019), task-state
115 FC has been shown to be quantitatively different from rsFC as task-evoked signals may assert
116 downstream effects on the correlation pattern of background brain regions (i.e. brain regions that
117 are hypothesized to not be directly influenced by the fMRI task) (Al-Aidroors et al., 2012) or
118 drive coincidental increases in the correlation patterns across brain regions that are otherwise
119 absent at rest (Cole et al., 2019). While the implication of not removing the task evoked signals
120 deserves further investigation, this study prioritizes its focus on the behavioral prediction
121 performance of these FC measures.

122 If the task effect, estimated by the task model fit of subject-level general linear models
123 (GLM) of task conditions, is removed (Arfanakis et al., 2000; Fair et al., 2007), the FC measures,
124 which we label the *task-model-residual FC*, capture the FC of the component of the task fMRI
125 time series that is not explained by the task design. The task-model-residual FC has also been
126 called “pseudo resting-state connectivity” (Jurkiewicz et al., 2018), “task FC” (Cole et al., 2014),
127 “task-based FC” (Cole et al., 2019), and “background connectivity” (Al-Aidroors et al., 2012) in
128 the literature. Because of its task-invariant nature, task-model-residual FC patterns have indeed

129 been shown to resemble rsFC patterns (Jurkiewicz et al., 2018; Cole et al., 2019) and are
130 predictive of behavioral differences across individuals (O'Halloran et al., 2018; Varangis, Habeck
131 & Stern, 2020). If the task-model-residual FC does capture the same functional brain
132 organization as resting-state FC as previous studies suggest (Jurkiewicz et al., 2018; Cole et al.,
133 2019), the reported superior behavioral prediction of the task-state FC over rsFC may be
134 attributable to the task effects that were removed from the task-model-residual FC. The task
135 effects that are being removed from the task-model-residual time series are estimated with GLM
136 models, where the beta estimates of task onsets and their temporal derivatives, which we refer to
137 as the *task model parameters*, capture the effect of task conditions on the time series of each
138 ROI. We can manipulate data from fMRI tasks to study the behavioral sensitivity of the FC
139 pattern of the task effects. By estimating the FC of the task model fit, which we call the *task-*
140 *model-fit FC*, we can directly assess and compare its behavioral relevance against the task-
141 model-residual FC, the task-based FC, and the rsFC. These comparisons generate new
142 hypotheses on the source of behavioral relevance in the task fMRI data and can provide
143 additional information to guide the optimization of fMRI paradigms for the investigation of
144 behavioral phenotypes.

fMRI paradigm	Measure name	Definition	Name in other studies
Resting-state fMRI	rsFC	Pairwise correlation of fMRI activity at rest	
fMRI tasks	Task-based FC	Pairwise correlation of the complete preprocessed task fMRI time series.	"Task-based FC" (Greene et al., 2018; Gao et al., 2019)

	Task-model-fit FC	<p>Pairwise correlation of task-model-fit time series which is the task fMRI time series component explained by the task design.</p> <p>The task-model-fit time series is derived by multiplying the task design matrix by the beta estimates of the task condition regressors and their temporal derivative.</p>	--
	Task-model-residual FC	<p>Pairwise correlation of the task-model-residual time series which is the task fMRI time series component that cannot be explained by the task design.</p> <p>The task-model-residual time series is derived by subtracting the task-model-fit time series from the preprocessed task fMRI time series.</p>	<p>"Pseudo resting-state connectivity" (Jurkiewicz et al., 2018) "Task FC" (Cole et al., 2014) "Task-state FC" (Cole et al., 2019) "Background connectivity" (Al-Aidroos et al., 2012)</p>
	Task model parameters	<p>The beta estimates of the task condition regressors and their temporal derivative derived from subject-level GLM models.</p>	

145 Table 1. Glossary for fMRI measures used in this study.

146 In this study, we leveraged the large sample of the Adolescent Brain Cognitive
147 Development (ABCD) Study ® and compared the behavioral prediction performance of rsFC to
148 the task-model-fit FC, task-model-residual FC, and task-based FC derived from the Emotional N-
149 back (nBack) task, the Stop Signal Task (SST), and the Monetary Incentive Delay (MID) task.

150 We evaluated the out-of-sample prediction performance of each FC measure on three behavioral
151 measures. The trait-like behavioral measure of interest was a measure of general cognitive
152 performance, the total composite cognitive score of the NIH Cognition Toolbox. As examples of
153 a more proximal, state-sensitive, behavioral measure we chose a behavioral inhibition measure
154 derived from the SST fMRI task, the stop-signal reaction time (SSRT), and a working memory
155 performance measure derived from the the nBack fMRI task, the 2-back accuracy measure. The
156 behavioral prediction of the task model parameters, the beta estimates of the task condition
157 regressors, was also estimated and contrasted with all task-derived FC measures. We also
158 quantified how the prediction performance of FC measures changed with the amount of usable
159 data and across sociodemographic variables, which are known to be associated with individual
160 variability in cognitive (Korous et al., 2020) and brain outcomes (Farah, 2018; Taylor et al.,
161 2020).

162 **2. Methods**

163 **2.1 Participants**

164
165 The ABCD Study is a longitudinal neuroimaging study that tracks brain and behavioral
166 development of 11,880 children starting at 9 and 10 years old. The ABCD study used school-
167 based recruitment strategies to create a demographically and ethnically diverse cohort (Garavan
168 et al., 2018) with an embedded twin cohort and many siblings. Informed consent was obtained
169 from parents/caretakers and assent was obtained from the children. Extensive descriptions of the
170 recruitment, collection, and processing of the fMRI and the behavioral data of the ABCD study
171 can be found in prior publications (Gavaran et al., 2018; Casey et al., 2018; Hagler et al., 2019).
172 Participants with complete data across all the behavioral measures and covariates of interest were
173 included in the analyses. To ensure accurate characterization of the FC matrices, participants

174 were required to have at least 50% of usable data for each of the two runs of each fMRI task, and
175 for each of the four resting state fMRI runs. The nBack task had the least number of participants
176 that met the inclusion criteria (n = 3034). In order to match the number of participants across
177 fMRI acquisitions for the behavioral prediction analysis, we randomly selected 3034 participants
178 from each of the other fMRI acquisitions. Around 25% of the participants are shared between the
179 final sample of each acquisition. The additional inclusion criteria and their effect on sample size
180 is shown in Supplementary Table 1.

181 [2.2 Behavioral measures](#)

182 Here, we describe the behavioral measures used in the present study. The full
183 neurocognition battery for the ABCD Study is detailed elsewhere (Luciana et al., 2018). The
184 NIH Toolbox Cognition Battery measures a range of cognitive domains that show substantial
185 development during childhood and adolescence. It consists of seven subtests, including measures
186 of vocabulary size (Picture Vocabulary Task), single word reading ability (Oral Reading Task),
187 rapid visual processing (Pattern Comparison Processing Speed Test), working memory capacity
188 (List Sorting Working Memory Test), episodic memory (Picture Sequence Memory Test),
189 attention and inhibitory control (Flanker Task), and cognitive flexibility (Dimensional Change
190 Card Sort Task). The composite measure of the NIH Toolbox Cognition Battery, the Total
191 Composite Score is an arithmetic average of the 7 subtests summarizing the cognitive
192 performance of an individual across the different cognitive domains. The age-uncorrected score
193 of the composite measure, the total composite cognition score, was used as a primary behavioral
194 outcome of this study. In the ABCD Study, participants perform the Stop Signal Task (SST)
195 during fMRI scans. In this task, participants are instructed to inhibit a prepotent motor response
196 to a Go Stimulus in response to a stop signal. A tracking algorithm varies the interval between

197 the onset of the Go stimulus and the onset of the Stop stimulus (the Stop Signal Delay) based on
198 individual performance. The Stop Signal Reaction Time (SSRT) quantifies the speed of the
199 inhibitory process during the SST task, such that lower SSRT reflects more efficient response
200 inhibition. The SSRT was calculated by subtracting participants' mean stop signal delay (SSD)
201 from their mean reaction time during the SST fMRI task. The 2-back accuracy, derived from the
202 nBack fMRI task, quantifies participants' working memory performance with participants'
203 average accuracy on all 2-back conditions across two nBack runs. We chose the SSRT and the 2-
204 back accuracy as additional behavioral outcomes because both measures quantify the
205 performance of a specific cognitive processes during an fMRI task, in contrast to the general
206 cognitive abilities assessed by the total composite cognition score. In addition, the measure was
207 derived directly from performance during the task fMRI session enabling us to assess links
208 between task performance and the miscellaneous FC measures obtained during that task.

209 [2.3 Resting-state and task fMRI paradigms](#)

210 The neuroimaging paradigms and acquisition parameters are detailed elsewhere (Casey et
211 al., 2018), so a brief overview is provided here. Four 5-minute resting-state fMRI runs were
212 acquired during which participants were instructed to fixate on a crosshair. Three task fMRI
213 acquisitions were completed after the resting-state fMRI, with two runs of each of the following
214 tasks: Emotional N-back task (nBack), Stop Signal Task (SST), and Monetary Incentive Delay
215 Task (MID). The order of the tasks was counterbalanced across participants. These tasks have
216 been shown to elicit anticipated patterns of brain activation in the ABCD Study baseline data
217 consistent with previous literature (Chaarani et al., 2021).

218 The nBack engages the neural correlates of working memory and emotional regulation
219 processes. To engage working memory, the task includes 0-back and 2-back conditions,

220 presented in a block design. For the 2-back condition, participants were instructed to indicate
221 with a button press whether the current stimulus matched the stimulus presented 2 trials back.
222 For the 0-back condition, a target stimulus was presented at the beginning of the block and
223 participants were instructed to press the button when they saw the target. To engage emotion
224 regulation, the task stimuli included happy faces, fearful faces, neutral faces, and places,
225 presented serially.

226 The SST engages the neural correlates of impulsivity and inhibitory control. In an event-
227 related design, participants were instructed to indicate the direction of a leftward or rightward
228 pointing arrow as quickly as possible. In 16.67% of the trials, the arrow was followed by a stop
229 signal represented as an upward arrow, and participants were instructed to withhold their
230 response. A tracking algorithm that varied the onset of the stimulus and the onset of the stop
231 stimulus (the stop signal delay, SSD) was implemented to ensure approximately 50% successful
232 and 50% unsuccessful stop trials.

233 The MID probes the neural correlates of reward processing. For each trial, participants
234 could either win money, lose money, or earn nothing. Wins and losses were further subdivided
235 into small or large amounts. At the start of each trial, participants were prompted with an
236 incentive cue of five possible trial types (win \$0.20, Win \$5, Lose \$5, Lose \$0.20, \$0-no money
237 at stake) followed by a jittered anticipation period, during which participants fixated on a
238 crosshair. Next, a target appeared to which participants made their button response. The trial
239 ended with positive or negative feedback to inform participants about their performance. Since
240 the MID task uses an adaptive algorithm that tracks to the performance of each participant, the
241 behavioral outcome measures (e.g. reaction time) are not comparable across participants. As a
242 result, no behavioral data from the MID task was used in this study.

243 2.4 Image acquisition and processing

244 2.4.1 Task and resting-state MRI acquisition and preprocessing

245 The ABCD MRI data were collected across 21 research sites using GE 750, Siemens
246 Prisma, and Philips Achieva and Ingenia 3T scanners. Scanning protocols were harmonized
247 across sites. The full details of the ABCD imaging acquisition and preprocessing protocols were
248 described in Casey et al. (2018) and Hagler et al. (2019). Briefly, T1w sMRI images (1mm
249 isotropic) were acquired with a 3D T1w inversion prepared RF-spoiled gradient echo scan, and
250 fMRI acquisitions (rest and task) were collected with multiband EPI with slice acceleration
251 factor 6 (2.4 mm isotropic, TR = 800ms). The preprocessing steps for fMRI data included (i)
252 head motion correction, (ii) B0 distortion correction, (iii) gradient warping correction, (iv)
253 within-scan motion correction, and (v) registration to T1w structural images. Initial frames
254 (Siemens and Philips scanners: 8 TRs; GE DV25: 5 TRs; GE DV26: 16 TRs) were removed
255 from the preprocessed task fMRI time course. Motion estimates were filtered to remove the
256 effect of respiratory signals (Fair et al., 2018). The preprocessed time courses were normalized
257 and sampled onto the cortical surface for each participant. Average time courses were calculated
258 for a functionally defined parcellation scheme (Gordon et al., 2016) sampled from the atlas-space
259 to individual subspace, and anatomically defined subcortical ROIs (Fischl et al., 2002).

260 2.4.2. Task model parameters, task-based fMRI time series, task-model-fit, and task-model- 261 residual time series estimation

262 The task effects were estimated at the participant level using a GLM that included the
263 stimulus timing for each task condition (Hagler et al., 2019) and the temporal derivative to
264 capture any task related changes in the fMRI time course that is not captured by our task model.
265 The GLM modeled each task condition with a bivariate gamma function and its first temporal

266 derivative along with 4 nuisance regressors for baseline shifts and cubic trends and 12 regressors
 267 for the six motion estimates and their temporal derivatives. For the GLM estimation, time points
 268 with framewise displacement (FD) greater than 0.9 mm were censored (Siegel et al. 2014). For
 269 the behavioral prediction response of the task model parameters, both the beta estimates of the
 270 task condition regressors and the temporal derivative were included as predictors.

271 The task-based time series was the task fMRI time series after preprocessing. The task-
 272 model-fit time series was the component of the preprocessed task fMRI time series that was
 273 explained by the task design and was calculated by multiplying task design matrix to the beta
 274 estimates of task condition regressors and their temporal derivative. The task-model-residual
 275 time series was the component of the preprocessed task fMRI time series that was not explained
 276 by the task, calculated by subtracting the task-model-fit time series from the preprocessed task-
 277 based time series.

278 In matrix expression, $Y_{tr,roi}$ is the observed fMRI time series matrix of an fMRI task with
 279 tr as the number of TRs and roi as the number of ROIs. $X_{roi,cond}$ describes task condition onset at
 280 each ROI with $cond$ as the number of task conditions. β is a $cond$ by roi task model parameters
 281 matrix that quantifies the effect of each task condition. The task model parameters, β , were
 282 estimated as:

283
$$\hat{\beta} = X^{-1} Y ,$$

284 which estimated the effect of the task condition onset on the observed time series.

285 The task-model-fit time series matrix, \hat{Y} , was estimated as:

286
$$\hat{Y} = X^{-1} \hat{\beta} ,$$

287 and \hat{Y} represented the estimated time series data at each ROI predicted by the task
288 condition onset. The task-model-residual time series matrix was estimated with:

289
$$\hat{\varepsilon} = Y - \hat{Y},$$

290 which summarized the component of the observed time series that could not be explained
291 by the task conditions.

292 The $\hat{\beta}$ corresponded to the task model parameters for behavioral prediction. The
293 correlation of the estimated task-model-fit time series, \hat{Y} , corresponded to the task-model-fit FC.
294 The correlation of the task-model residuals, $\hat{\varepsilon}$, corresponded to the task-model-residual FC. The
295 correlation of the observed time series, Y , corresponded to the task-model-residual FC.

296 2.4.3 FC estimation

297 Several additional preprocessing steps were applied to the resting-state and task fMRI
298 time series before the estimation of FC to reduce spurious signals that are unlikely to reflect
299 functional brain activation. These steps included (1) censoring and residualization and removal
300 of signals associated with cerebral white matter, ventricles, whole brain, and head motion
301 estimates and their squares and derivatives (Power et al., 2014; Satterthwaite et al., 2012), (2)
302 motion regression where frames with FD over 0.3mm were excluded (Power et al., 2014), and
303 (3) band-pass filtering (0.009 and 0.08 Hz) (Hallquist et al., 2013). Motion traces were
304 temporally filtered using an infinite impulse response (IIR) notch filter and the cutoffs are 0.31
305 and 0.43 Hz. Additional motion censoring was applied to exclude the following time points: time
306 points with FD over 0.2mm, time points that were outliers with respect to the spatial variation
307 across the brain, and time periods with less than 5 contiguous, sub-threshold time points.
308 Average time courses were calculated for 333 cortical ROIs (Gordon et al., 2016) and 19

309 subcortical ROIs (Fischl et al., 2002) for each run and were concatenated. Pearson correlations
310 were applied to calculate the pairwise correlations of these 352 ROIs. The r-to-z transformed
311 correlation matrix formed the FC estimate of each time series.

312 2.5 Statistical analysis

313 2.5.1 Behavioral prediction algorithm

314 A nested 10-fold cross validation scheme was used to estimate the out-of-sample
315 prediction performance of each set of fMRI measures. Participants from the same family were
316 kept within the same training and testing set during the cross validation. Within each training set,
317 the mass univariate beta estimates between each fMRI measure and a behavior were estimated
318 using the Fast Efficient Mixed Effects Analysis (FEMA; Fan et al., 2021) where a general linear
319 mixed effects model was estimated at each voxel or ROI. Compared to the traditional general
320 linear models, FEMA explicitly adjusts for the effects of the nested family structure in the ABCD
321 data and the covariates of no interest. The following sociodemographic and imaging acquisition
322 variables were included in the FEMA models as covariates: age, biological sex, top 10 genetic
323 PCs, highest parental education, household income, scanner ID (MRI device serial number) and
324 software version. Mean framewise displacement (FD) and the number of usable time points were
325 used as additional covariates for FC measures. A separate analysis was conducted without the
326 inclusion of sociodemographic variables as covariates to probe the shared impact of
327 sociodemographic variables on the imaging and the behavioral measure. For this analysis, only
328 scanner ID and software version were used as covariates, along with mean FD and the number of
329 usable time points for FC measures.

330 For behavioral prediction, the mass univariate beta estimates from FEMA were entered
331 into a singular-value decomposition (SVD) based prediction method to predict the behavioral

332 outcome of the unseen, test-set participants. Similar to our previous method, the Bayesian
333 polyvertex score (PVS_B, Zhao et al., 2021), the SVD-based prediction method applies shrinkage
334 to the mass univariate beta estimates to improve out-of-sample prediction performance. The
335 shrinkage factor was derived separately for each brain-behavior association with a 5-fold cross
336 validation nested within each training set. Within each nested training set, SVD was applied to
337 the imaging measure pre-residualized for sociodemographic covariates to approximate the
338 covariance structure of the mass univariate beta estimates. From the SVD result, the top k
339 singular vectors and their corresponding singular values were used to calculate a shrinkage factor
340 that was used to reweight the mass univariate beta estimates from FEMA. One hundred k values
341 were selected at equal distances between 1 and the dimension of the predictor space. The best
342 performing k value was selected as the shrinkage factor for the full training set. The reweighted
343 mass univariate estimates were then applied to the test set imaging data to calculate the predicted
344 behavioral score for each test set participant. A separate cross validation procedure that was
345 based on ABCD sites (i.e. leave-one-site-out) was also implemented (see S.I. Methods) to
346 examine the effect of the chosen cross validation procedure on behavioral prediction.

347 The predicted behavioral score summarizes the variability in the behavioral outcome that
348 is attributable to individual differences of the imaging measure. Squared correlation between the
349 predicted and the observed behavioral score was used as the metric for out-of-sample behavioral
350 prediction performance of each imaging measure. The ninety-five percent confidence interval of
351 the behavioral prediction performance of each fMRI measure was generated with bootstrap
352 resampling (Elliot et al., 2019) using the `ci_cor` function (`confintr` package) in R. The predicted
353 behavioral scores were also used in subsequent analyses to probe the shared and unique
354 behavioral variance explained by different FC measures.

355 All usable data from each modality were included in the behavioral prediction analysis.
356 As resting-state fMRI was collected with 4 runs while the task-fMRI was collected with 2 runs of
357 data, we investigated how the behavioral prediction performance of each FC measure was
358 affected by scan length, i.e. the number of runs in supplementary analysis (Supplementary
359 Methods).

360 2.5.2 Quantification of shared and unique behavioral variance explained by the task-model-fit FC 361 and the task-model-residual FC

362 As the task-model-fit FC and task-model-residual FC were derived as complementary
363 subcomponents of the same task fMRI time series, we examined if they contained unique
364 information for behavioral differences by estimating their shared and unique behavioral variance
365 explained. In this set of analysis, we used the predicted behavioral scores of each FC measure on
366 each behavior as the predictor because they captured the prediction effects of FC measures on
367 behaviors while reducing the predictor dimensionality to a single measure. We first estimated the
368 out-of-sample behavioral prediction performance of the predicted behavioral scores of task-
369 model-fit FC and of the task-model-residual FC individually with generalized additive mixed
370 models (GAMMs) with sociodemographic factors as fixed effects covariates and family ID as
371 random effects. These *univariate models*, with only one brain predictor in the model, gave us an
372 estimate of the behavioral variance explained by each FC in isolation. Then, we estimated their
373 total prediction effect by including the predicted behavioral scores of both FC measures as
374 predictors in an *augmented model*, with sociodemographic factors as fixed effects covariates and
375 family ID as random effects.

376 The unique variance explained by the task-model-fit FC (unique R^2 adjusted for task-
377 model-residual FC) was calculated as the difference in R^2 between the univariate model with the

378 predicted behavioral score of the task-model-residual FC as the only FC predictor and the
379 augmented model with the predicted scores of both the task-model-fit FC and the task-model-
380 residual FC. The unique variance explained by the task-model-residual FC (unique R^2 adjusted
381 for task-model-fit FC) was estimated as the difference in R^2 between the univariate model with
382 the predicted behavioral score of the task-model-fit FC and the augmented model. The gamm4
383 (gamm4 package) function was used to perform GAMMs in R and the r.squaredGLMM (MuMIn
384 package) function was used to estimate the behavioral variance explained (fixed effects pseudo-r-
385 squared) of the fMRI predictors from GAMMs.

386 2.5.3 Quantification of shared and unique behavioral variance explained by the task-model-fit FC 387 and the task model parameters

388 Both task-model-fit FC and task model parameters capture the task effects on brain
389 activity. We assessed whether these two task effects measures explained unique behavioral
390 variance by quantifying the shared and unique variance explained of the predicted behavioral
391 scores of the task-model-fit FC and the task model parameters. An augmented model that
392 included both measures was performed to estimate the total prediction effect of the task-model-fit
393 FC and the task model parameters. The unique variance explained by the task-model-fit FC
394 (unique R^2 adjusting for task model parameters) was estimated as the difference in R^2 between
395 the augmented model and the univariate model with task model parameters. The unique variance
396 explained by the task model fit (unique R^2 adjusting for task-model-fit FC) was estimated as the
397 difference between the augmented model and the univariate model with task-model-fit FC.
398 Family relatedness was modeled as a random effect and sociodemographic factors were used as
399 fixed effects covariates for all the above-mentioned models.

400 2.5.4 The effect of sociodemographic factor adjustment on behavioral prediction performance

401 To understand how sociodemographic factor adjustment changes the behavioral
402 prediction performance of fMRI measures, we reran the above behavioral prediction models
403 without the adjustment of sociodemographic factors and only including scanner ID, scanner
404 software version, mean FD, and the number of usable timepoints as covariates in FEMA. The
405 unadjusted mass univariate beta estimates of all FC and task model parameters were used to
406 calculate the behavioral prediction performance of all fMRI measures without the adjustment of
407 sociodemographic differences in our sample. The prediction performance of each fMRI measure
408 with and without sociodemographic adjustment was compared.

409 2.6 Data Statement

410 Data used in this article were obtained from the Adolescent Brain Cognitive
411 Development (ABCD) Study (<https://abcdstudy.org>), held in the NIMH Data Archive (NDA).

412 3. Results

413 3.1 Task-model-fit FC and task-based FC conferred task-specific advantage at predicting 414 individual differences in behavior over rsFC and task-model-residual FC.

415 Prediction performance of rsFC and the three task-derived FC measures on individual
416 differences in total composite cognition score, SSRT, and 2-back accuracy are shown in Figure
417 1. After adjusting for sociodemographic variables, the squared correlation between the rsFC and
418 the total composite cognition was 0.036. The squared correlations between the nBack, SST, and
419 MID task-model-residual FC estimates and the total composite cognition were 0.033, 0.021, and
420 0.034, respectively.

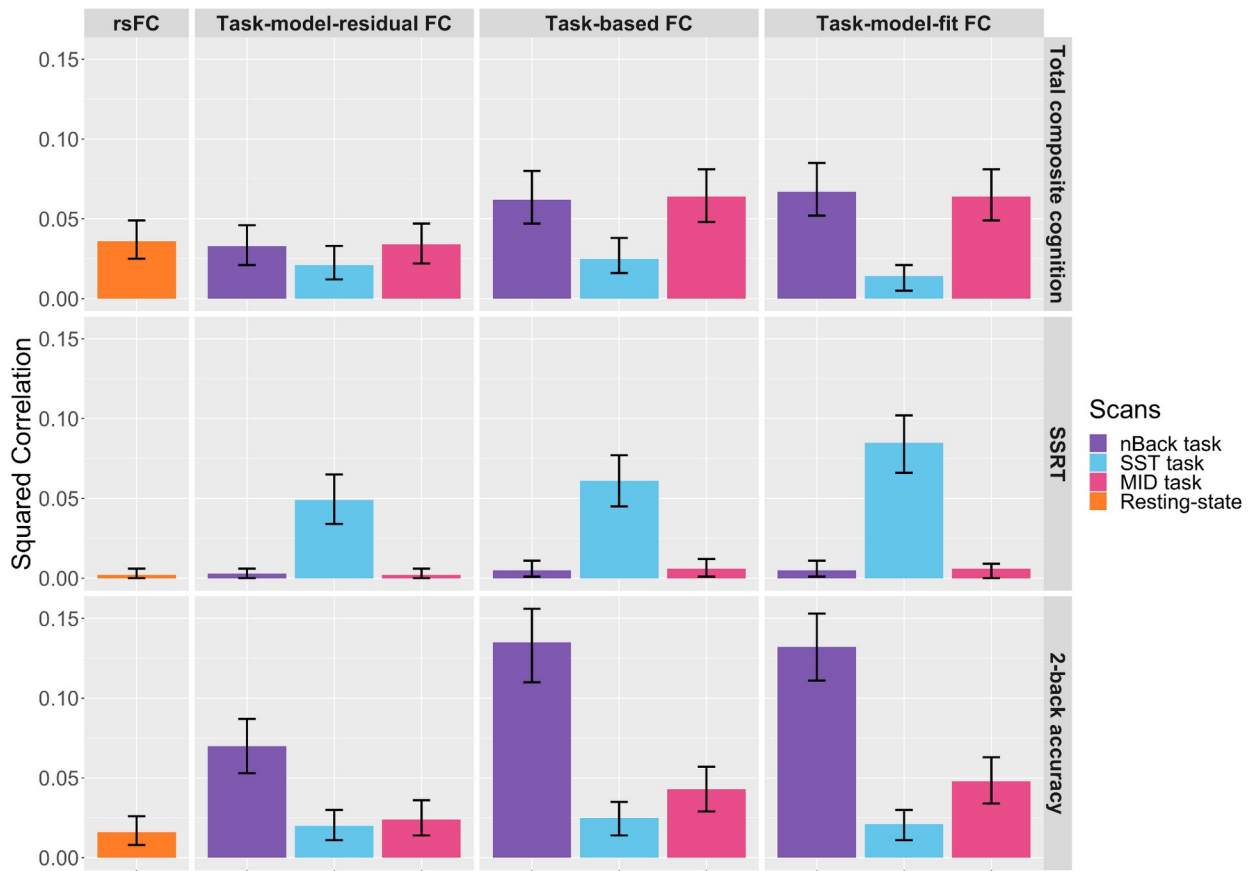
421 Increased behavioral prediction was observed for the task-based FC and the task-model-
422 fit FC derived from the nBack and the MID task. The squared correlations between the total
423

424 composite cognition and the nBack task-based FC and task-model-fit FC were 0.062 and 0.067,
425 and the squared correlations of the MID task-based FC and task-model-fit FC were 0.064 and
426 0.064. We did not observe an increase in prediction for the SST task-based and the task-model-fit
427 FC on total composite cognition (SST task-model-fit FC squared correlation: 0.014; SST task-
428 based FC squared correlation: 0.025). Behavioral prediction performance of fMRI measures
429 estimated using leave-one-site out cross validation followed similar patterns as the 10-fold cross
430 validation.

431 We observed a task-specific effect of SST-derived FC measures on SSRT. Only FC
432 measures derived from the SST task were significantly predictive of the individual differences in
433 SSRT. Among the SST task FC measures, we observed an advantage for the SST task-model-fit
434 FC relative to the SST task-model-residual FC. The squared correlation between the SST task-
435 model-fit FC and SSRT was 0.095, while the squared correlation of the SST task-model-residual
436 FC was 0.049. We compared the FEMA z-score map of the SST task-model-residual FC on
437 SSRT to the effect size map of the SST task-model-fit FC, the SST task-based FC, and the rsFC
438 (Figure 2). The mass univariate beta estimates of the SST task-model-residual FC bore greater
439 resemblance to the effect size map of the SST task-model-fit FC than to the rsFC, suggesting that
440 the SST task-model-residual FC captured a similar predictive pattern as the SST task-model-fit
441 FC. The mass univariate beta estimates of other brain-behavior associations are shown in
442 Supplementary Figures (SI. Figure 1-4).

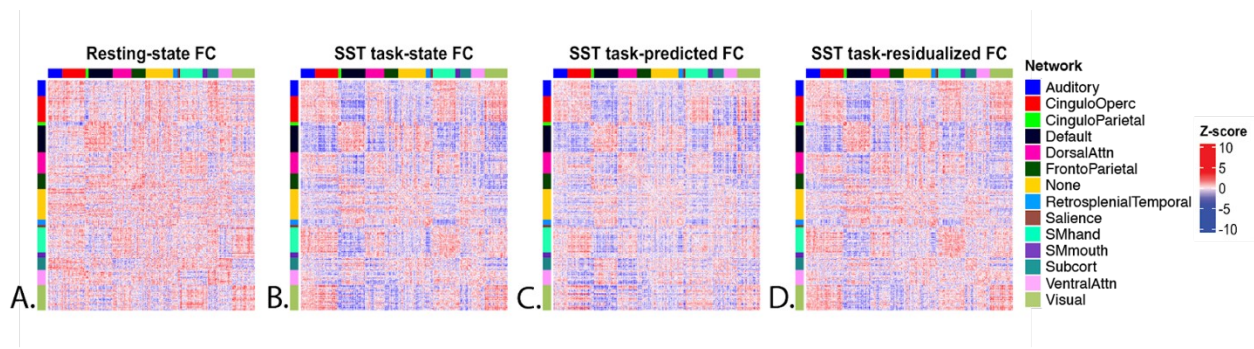
443 A similar task-specific advantage was also observed for the nBack FC measures at
444 predicting 2-back accuracy. While the squared correlation between the rsFC and the 2-back
445 accuracy was 0.016, the squared correlations of the nBack task-model-residual FC, the nBack
446 task-state FC, and the nBack task-model-fit FC were 0.07, 0.135, and 0.132, respectively. The

447 FC measures derived from the SST task demonstrated similar prediction performance as the
 448 rsFC. For the MID task, we also observed a greater association between the MID-derived FC
 449 measures and the 2-back accuracy than the rsFC and the SST-derived FC measures. The squared
 450 correlations of the MID task-model-residual FC, task-state FC, and task-model-fit FC were
 451 0.024, 0.046, and 0.048, respectively.



452
 453 Figure 1. The task-based FC and task-model-fit FC outperformed rsFC and task-model-residual
 454 FC at predicting individual variability in total composite cognition, SSRT, and 2-back accuracy.
 455 For total composite cognition (top row), rsFC (first column) and the task-model-residual FC
 456 measures (second column) showed similar behavioral prediction performance. Task-based FC
 457 (third column) and task-model-fit FC (fourth column) of the nBack and MID task, on the other
 458 hand, outperformed rsFC and task-model-residual FC explaining behavior differences in total

459 composite cognition. For the SSRT (middle row), only task-derived FC measures from the SST
 460 task were predictive. All SST task FC measures were predictive of the SSRT, while rsFC was
 461 not. For the 2-back accuracy (bottom row), the nBack-derived task FC measures outperformed
 462 the rsFC and the task-derived FC measures from the other two fMRI tasks. Error bars show the
 463 ninety-five percent confidence intervals estimated with bootstrap resampling.



464
 465 Figure 2. The effect size matrices of the SST task FC measures on SSRT were more similar to
 466 each other than to rsFC. 352 ROIs x 352 ROIs effect size matrices, organized by functional
 467 network, are shown. Each cell corresponds to the mass univariate z-score of each ROI pair on
 468 SSRT derived from FEMA analyses.

469 We conducted post-hoc correlation analyses on the behavioral outcome variables to
 470 examine whether the task-specific advantage of the nBack and the SST task was due to a high
 471 correspondence between the in-scanner cognitive behaviors and out-of-scanner behavioral
 472 outcomes. If the in-scanner behavior of an fMRI task is highly correlated with the out-of-scanner

473 behavior of interest, we expect to observe that that fMRI task is better at predicting the out-of-
474 scanner behavior of interest.

475 The correlation between the total composite cognition, SSRT, and the 2-back accuracy
476 was estimated in the sample of participants who were sampled for the rsFC prediction analysis.
477 The 2-back accuracy measure was highly correlated with the total composite cognition ($r = 0.46$)
478 but not with SSRT ($r = -0.07$). This could contribute to the greater prediction performance of the
479 nBack-derived FC measures on total composite cognition. The SSRT, on the other hand, was not
480 positively correlated with either the total composite cognition ($r = -0.12$) or the 2-back accuracy.
481 This lack of in-scanner behavior and out-of-scanner behavior correlation might contribute to the
482 minimum association between the SST-derived FC measures and the other behavioral measures.

483 [3.2 Task-model-fit FC accounted for the behavioral variance predicted by the task-model-
484 residual FC.](#)

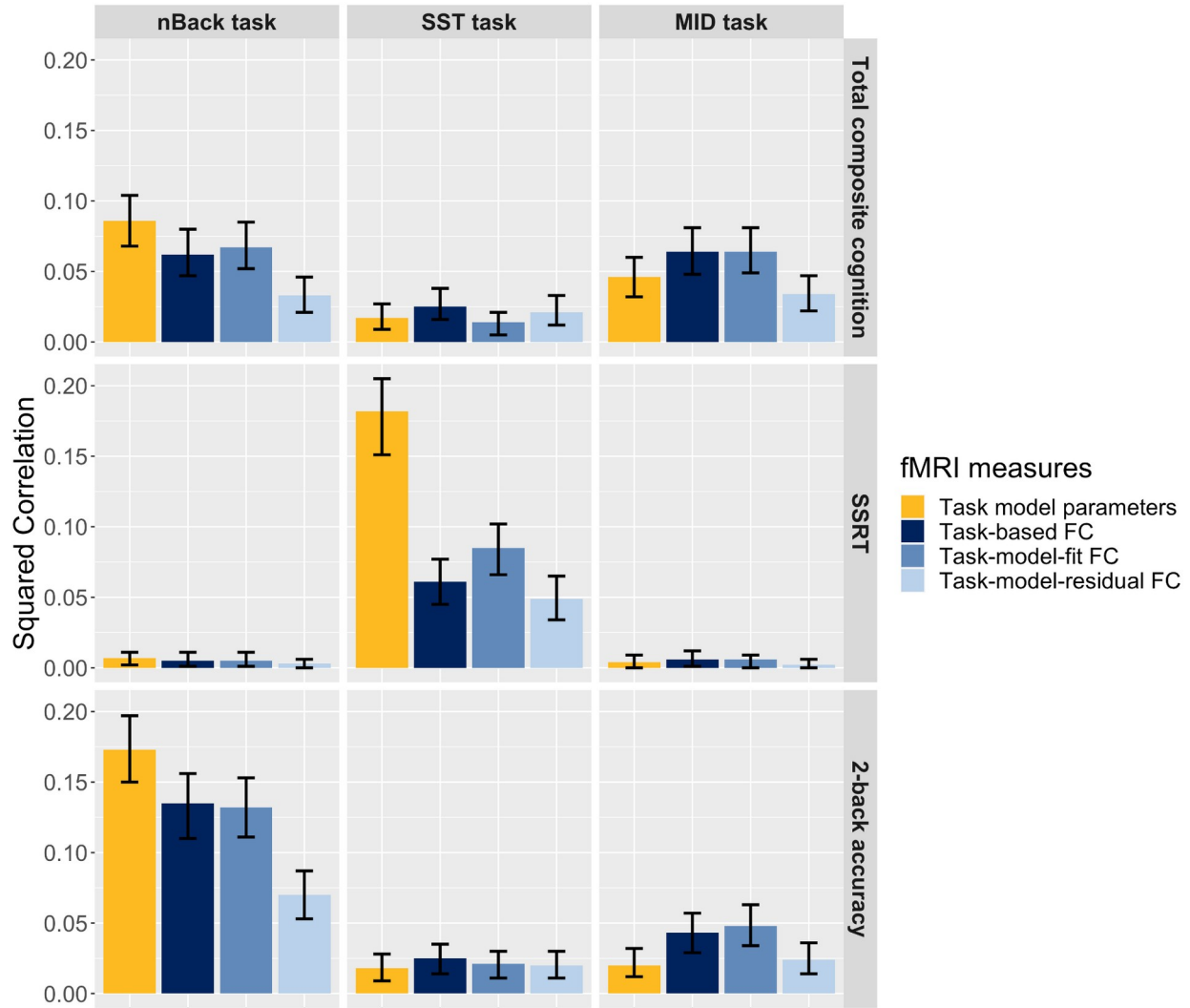
485 Given that the task-model-fit FC and task-model-residual FC were derived from
486 complementary subcomponents of the task fMRI time series, we examined whether these FC
487 measures contributed unique information to behavioral prediction (Table 2) by quantifying the
488 shared and unique variance explained by the predicted behavioral scores of the two FC measures.
489 For the prediction of total composite cognition by the nBack and MID tasks, task-model-residual
490 FC contributed minimal unique variance explained ($R^2 < 1\%$) after adjusting for task-model-fit
491 FC. On the other hand, the nBack and MID task-model-fit FC each explained 4.1% variance in
492 total composite cognition after adjusting for task-model-residual FC. Therefore, task-model-fit
493 FC predicted unique behavioral variance, while task-model-residual FC did not. By contrast,
494 SST task-model-fit FC did not contribute unique variance to predicting total composite
495 cognition, while the SST task-model-residual FC uniquely explained 1.3% of the variance. For

496 the SST-SSRT association, after adjusting for the shared behavioral variance explained, both the
 497 SST task-model-fit FC and the SST task-model-residual FC predicted unique variance in SSRT
 498 (SST task-model-fit FC: unique $R^2 = 4.5\%$; SST task-model-residual FC: unique $R^2 = 1.1\%$). We
 499 believe that the unique association between SSRT and the SST task-model-residual FC might be
 500 attributable to the insufficient modeling and removal of the SST task effect. For the prediction of
 501 2-back accuracy, both nBack task-model-fit FC and the nBack task-model-residual FC predicted
 502 unique behavioral variance, although the unique variance explained by the task-model-fit FC was
 503 much greater than the task-model-residual FC (nBack task-model-fit FC: unique $R^2 = 7.9\%$;
 504 nBack task-model-residual FC: unique $R^2 = 1.8\%$).

fMRI tasks	Task-model-fit FC		Task-model-residual FC	
	R^2	Unique R^2 adjusted for task- model-residual FC	R^2	Unique R^2 adjusted for task-model-fit FC
<i>Behavior: Total composite cognition</i>				
nBack	6.4%	4.1%	3.1%	0.8%
SST	1.1%	0.4%	2.0%	1.3%
MID	6.6%	4.1%	3.1%	0.6%
<i>Behavior: SSRT</i>				
nBack	0.4%	0.4%	0.2%	0.1%
SST	7.9%	4.5%	4.5%	1.1%
MID	0.2%	0.1%	0.3%	0.2%
<i>Behavior: 2-back accuracy</i>				
nBack	12.9%	7.9%	6.9%	1.8%
SST	1.9%	0.9%	1.9%	0.9%
MID	4.5%	2.6%	2.3%	0.3%

505 Table 2. The shared and unique variance explained (R^2) of the task-model-fit FC and the task-
 506 model-residual FC for each brain-behavior association.

507 3.3 Similar to the task-model-fit FC, task model parameters also exhibited a task-specific
 508 prediction advantage over the task-model-residual FC and rsFC.



509
 510 Figure 3. Task model parameters outperformed task-model-residual FC at predicting behavioral
 511 differences. Similar to the task-model-fit FC, task model parameters (yellow) demonstrated task-
 512 specific advantage over the task-model-residual FC at predicting total composite cognition (top
 513 row), SSRT (middle row), and 2-back accuracy (bottom row).

514 The task model parameters were equally, if not more predictive, than the task-model-fit
515 FC and significantly outperformed the task-model-residual FC (Figure 3) at predicting behavioral
516 differences. For total composite cognition, the nBack task model parameters were more
517 predictive than the nBack task-model-fit FC (squared correlation: 0.084), and the MID task
518 model parameters were less predictive of total composite cognition (squared correlation: 0.043).
519 For SSRT, the SST task model parameters showed the best predictive performance of all fMRI
520 measures (squared correlation: 0.182) and doubling the prediction effect of SST task-model-fit
521 FC. For 2-back accuracy, the nBack task-model-parameters (squared correlation: 0.167) again
522 outperformed the task-model-fit FC (squared correlation: 0.067). Across all task-derived FC
523 measures, the task-model-residual FC was the least predictive across all brain-behavioral
524 measures.

525 3.4 Task model parameters and task-model-fit FC explained both shared and unique behavioral 526 variance.

527 We next examined whether the task model parameters and task-model-fit FC offered
528 redundant functional brain information relevant for behavior by quantifying the unique
529 behavioral variance explained by the predicted behavioral score of each brain measure after
530 adjusting for the prediction effect of the other (Table 3). We observed a decrease in unique
531 variance explained (unique R^2) for both measures, suggesting that a proportion of the behavioral
532 association was shared between the task model parameters and the task-model-fit FC. Though
533 there was this decrease, both measures were uniquely associated with behavior, still explaining
534 meaningful variance after adjusting for the effect of the other measure. For example, the nBack
535 task model parameters explained 8% of the variance in total composite cognition. After adjusting
536 for the effect of the task-model-fit FC, it uniquely explained 3.1% of behavioral variance. The

537 nBack task-model-fit FC explained 6.4% of the behavioral variance in total composite cognition,
 538 and after adjusting for the effect of task model parameters, its unique R² dropped to 1.5%.

539

fMRI task	Task model parameters		Task-model-fit FC	
	R ²	Unique R ² adjusted for task-model-fit FC	R ²	Unique R ² adjusted for task model parameters
<i>Behavior: Total composite cognition</i>				
nBack	8.0%	3.1%	6.4%	1.5%
SST	1.5%	1.1%	1.3%	0.8%
MID	4.3%	1.7%	6.4%	3.9%
<i>Behavior: SSRT</i>				
nBack	0.5%	0.3%	0.4%	0.2%
SST	16.7%	11.6%	7.6%	2.5%
MID	0.3%	0.3%	0.4%	0.3%
<i>Behavior: 2-back accuracy</i>				
nBack	16.7%	6.6%	13.0%	2.9%
SST	1.6%	1.0%	2.0%	1.3%
MID	1.9%	0.5%	4.9%	3.4%

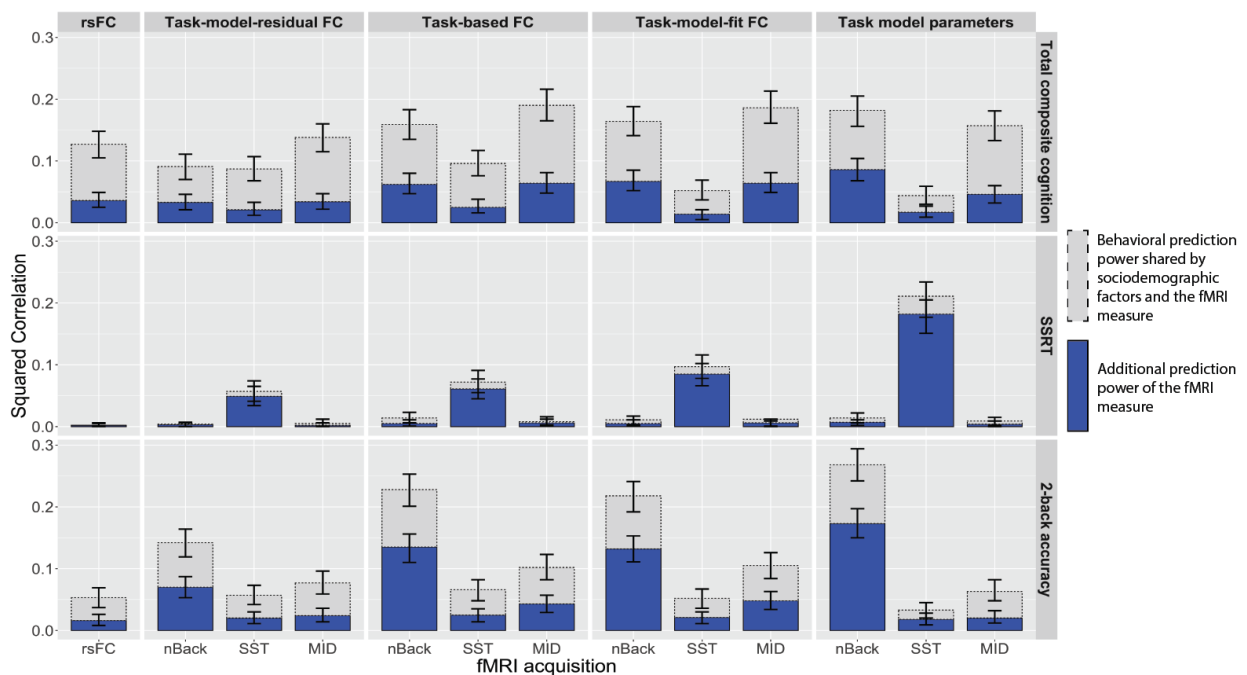
540 Table 3. Task model parameters and task-model-fit FC explained both shared and unique
 541 variance in individual differences in behaviors. The R² columns display the individual variance
 542 explained for each fMRI measure, corresponding to the data shown in Figure 1 and Figure 4. The
 543 R² adjusted columns display the unique variance explained after adjusting for the effect of the
 544 other fMRI measure.

545 [3.5 Adjusting for sociodemographic factors reduced the behavioral prediction performance of FC](#)
 546 [and task model parameters.](#)

547 Sociodemographic variables accounted for a proportion of the unadjusted behavioral
 548 association of fMRI measures, and the effect was more prominent for the prediction of total

549 composite cognition (Figure 4). When not controlling for sociodemographic factors, the squared
 550 correlation between rsFC and total composite cognition was 0.127. That number dropped to
 551 0.036 after the adjustment for sociodemographic differences. A similar reduction in prediction
 552 performance was observed for the task-derived FC measures and task model parameters. The
 553 prediction performance for 2-back accuracy also showed a significant reduction when adjusting
 554 for sociodemographic variables. For the association between the SSRT and the SST task, we
 555 observed a more moderate effect of sociodemographic adjustment. The SST task model
 556 parameters had a squared correlation of 0.211 with SSRT without the adjustment of
 557 sociodemographic covariates. After covarying for sociodemographic factors, its squared
 558 correlation was 0.182.

559



560

561 Figure 4. A proportion of the behavioral prediction power of task model parameters and FC

562 measures was explained by sociodemographic variation across individuals. The unadjusted

563 prediction squared correlation or each behavioral outcome, represented by the total height of the
564 bar, was partitioned into two components, a variance component that was shared with
565 sociodemographic factors (shown in gray) and a variance component that was additive to the
566 effect of sociodemographic factors (shown in blue), i.e., the prediction effect after adjusting for
567 sociodemographic covariates.

568 **4. Discussion**

569

570 Characterizing the optimal fMRI measures that capture variance in behavioral differences

571 is a critical step to develop reliable neuroimaging biomarkers for the detection and treatment of

572 brain and behavioral disorders. This study addressed this issue by comparing the behavioral

573 prediction performance of resting-state and task-derived fMRI measures including resting-state

574 FC, task-based FC, task-model-fit FC, task-model-residual FC, and task model parameters.

575 Previous findings have suggested that task fMRI is better than resting-state fMRI at capturing

576 behaviorally relevant FC signals (Rosenberg et al., 2016; Greene et al., 2018; Finn & Bandettini,

577 2021). We hypothesized that fMRI tasks better reproduce neural processes required to meet the

578 cognitive demands that individuals experience in real life and thus elicit changes in FC patterns

579 that are better associated with individual differences in behavioral phenotypes. We found that,

580 when an fMRI task captured similar cognitive constructs as the behavior of interest, task-model-

581 fit FC and task model parameters were better than rsFC and the task-model-residual FC

582 component at predicting individual differences in that behavior.

583 **4.1 Behavioral differences are better predicted by FC patterns derived from task fMRI than**

584 **resting-state fMRI.**

585 Consistent with previous findings (Rosenberg et al., 2016; Greene et al., 2018; Finn &
586 Bandettini, 2021), we observed an advantage for the task fMRI paradigms over resting-state
587 fMRI at predicting individual differences in both trait-level behavioral measures, such as the total
588 composite cognition, and state-level behavioral outcomes, such as the SSRT and 2-back
589 accuracy. This finding corroborates the previous result that task manipulation accentuates the
590 functional correlation patterns of the brain that are behaviorally relevant (Cole et al., 2021). This
591 behavioral prediction advantage of task-derived FC measures is also task-specific, such that only
592 fMRI tasks that evoke relevant cognitive demands and content to the behavior of interest confer
593 this advantage (Greene et al., 2018; Finn et al., 2017). In our study, this was demonstrated by the
594 double dissociation of the nBack and the SST task in the prediction of total composite cognition
595 and SSRT. We also found a greater association between 2-Back accuracy and the total composite
596 cognition, which could reflect that children with strong working memory abilities also performed
597 better on language tasks and tasks tapping into fluid intelligence (Rosenberg et al., 2020). A
598 previous study (Marek et al., 2022) has shown that the prediction advantage of fMRI tasks over
599 rest can be explained by the correlation between in-scanner task behaviors (e.g. working memory
600 during the nBack task) and the out-of-scanner behavior of interest (e.g. total composite
601 cognition). Consistent with what was found in Marek et al., we found there was a high
602 correlation between our in-scanner behavior (2-back accuracy) and out-of-scanner behavior (total
603 composite cognition). However, we do not believe this constitutes a confound as it has
604 previously been interpreted; rather, it helps explain why we see some generalizability of in-
605 scanner functional brain measures to out-of-scanner behavioral performance. Among all fMRI
606 modalities examined in this study, in-scanner behaviors of the resting-state fMRI (i.e. lying still
607 and staring at a crosshair) bore minimum resemblance with our behavioral measures of interest,

608 which might explain the moderate association between rsFC and all behavioral outcome
609 variables. While resting-state fMRI has been indispensable for the characterization of large-scale
610 brain networks and provides a convenient paradigm for cross-study data aggregation, task fMRI
611 might be a better vehicle to probe behaviorally relevant FC signals.

612 To assess the shared and unique information resided in different task-derived FC
613 measures, our analysis focused on comparing the shared and unique behavioral variance
614 explained by the task-model-fit FC and the task-model-residual FC as they are mutually
615 exclusive, subcomponents of the task-state FC. Our analysis showed that the behavioral
616 prediction advantage of task fMRI paradigms is driven by task-model-fit FC, that is, changes in
617 FC patterns in response to cognitive demand, and the task-model-residual FC, FC fluctuations
618 that are not explained by task demands, contributed little unique information at predicting
619 behavioral differences. While task-elicited FC fluctuations are modest compared to the
620 individual-specific functional connectome identified at rest (Laumann et al., 2017; Gratton et al.,
621 2018), these task-induced modulations improve the modeling and detection of behavioral
622 differences because they directly reflect changes in the functional brain patterns when a behavior
623 is being performed.

624 4.2 Task model parameters are equally, if not more predictive, than the task-model-fit FC, and
625 both measures confer complementary information on behavioral differences.

626 The task model parameters were equally, if not more predictive, than the task-model-fit
627 FC at predicting individual differences of both behavioral measures. The squared correlation of
628 the SST task model parameters and SSRT was 0.2, which is a significant improvement relative to
629 the SST task-model-fit FC, the best predicting FC measure from the same fMRI task. A similar
630 magnitude of prediction performance was achieved by the nBack task-model-parameters and the

631 2-back accuracy (squared correlation: 0.167). Despite the excitement of using FC measures to
632 behavioral differences in the literature, our results suggest that fMRI task activations are at least
633 as good, if not better, than FC measures at capturing individual differences in behavior.

634 We also showed that task model parameters and task-model-fit FC contained shared and
635 unique information for predicting behavioral differences, an observation consistent with previous
636 reports (Larabi et al., 2018; Kowalski et al., 2019). Characterizing the behavioral relevance of
637 both task fMRI measures allowed us to uncover unexpected behavioral association patterns with
638 fMRI tasks. For example, we did not expect to observe an association between the MID task FC
639 and the total composite cognition score given limited theories connecting the two measures.
640 However, we found that the MID task-model-fit FC was equally predictive of total composite
641 cognition score as the nBack task, a working memory task previously associated with cognitive
642 development (Sripada et al., 2020; but also see Kardan et al., 2022). This unexpected finding was
643 supported by studies reporting similar cognitive performance prediction accuracy for FC
644 measures derived from a working memory task and a reward processing task that captures
645 similar cognitive constructs as the MID task, in the Human Connectome Project (HCP) (Greene
646 et al., 2018; Jiang et al., 2020). As both the task model parameters and task-model-fit FC
647 measures can be readily derived from existing task fMRI data, we suggest future studies assess
648 the behavioral relevance of both, as they might yield additive information about the neural
649 correlates of complex behavioral phenotypes.

650 4.3 Sociodemographic factors treatment is crucial and yields differential implications for 651 behavioral prediction studies of fMRI measures

652 Importantly, we found that adjusting for sociodemographic covariates, including age, sex
653 at birth, ancestry, ethnicity, income, and education, significantly impacted the behavioral

654 prediction effect of FC measures and task model parameters, and such effects were more
655 prominent for total composite cognition and 2-back accuracy than for the SSRT. This is
656 consistent with previous findings that sociodemographic factors account for substantial
657 individual variability in fMRI phenotypes (Yaple & Yu, 2020; Rakesh, Zalesky, Whittle, 2021)
658 and in measures of cognitive performance (Bradley & Corwyn, 2002; Korous et al., 2020), and
659 that adjusting for sociodemographic factors reduces the effect sizes of rsFC measures on
660 cognitive task performance (Marek et al., 2022).

661 Controlling for sociodemographic factors can substantially alter estimates of the power of
662 brain phenotypes to predict behavioral differences. An investigator's choice to include these
663 variables as covariates, and which to include, should be guided by the specific prediction goal of
664 the analysis. Because sociodemographic variables are so robustly linked to both neuroimaging
665 and behavioral phenotypes in the ABCD Study, it will probably be necessary to consider the
666 pattern of associations across many models to begin to understand these underlying relationships.
667 Here we have chosen to present both the model with no adjustment and the model with
668 adjustment for all the sociodemographic variables listed above. For our predictions of the total
669 composite cognition score in the general population, the results suggest robust association
670 between this measure and functional brain phenotypes. However, the results with the full model
671 (including covariates) suggest that when only differences among peers of the same age, sex,
672 ancestry, ethnicity, and parental income/education are considered in the model, the associations
673 with functional brain phenotypes are much more modest. This trend was also observed in an
674 earlier study of ABCD participants involving structural brain phenotypes (Palmer et al. 2021).
675 While these discrepancies in the results can sometimes lead to confusion for scientists and other
676 stakeholders, it is important to emphasize that the different models both answer different

677 questions about prediction and raise new questions about the factors that reduce generalizability
678 across groups within the population. To address this uncertainty, it may be helpful for
679 researchers to develop standards for presenting several covariate models in each publication to
680 help readers understand better the context of their estimates of prediction from neuroimaging
681 phenotypes (see Wagenmakers et al., 2022).

682 4.4 Limitations

683 We used a correlation-based FC estimation framework to quantify the behavioral
684 relevance of resting-state and task fMRI data. Graph-theory derived network properties of FC
685 measures have also been associated with behavioral outcomes (Liu et al., 2012; Khazaei,
686 Ebrahimzadeh, Babajani-Feremi, 2015; Qian et al., 2018) and might have provided evidence for
687 additional prediction power. The out-of-sample behavioral prediction in this study could be an
688 underestimation of the behavioral relevance of resting-state fMRI and task fMRI data as other
689 network-based fMRI properties might introduce additional behavioral prediction power relative
690 to the correlation-based FC measures. This limitation, however, would not change our
691 conclusions regarding the relative advantage of task-related FC over rsFC for capturing
692 behaviorally relevant differences, as all FC measures were processed with the same censoring
693 and filtering criteria and were applied to the same prediction pipeline. Similarly, our choice of
694 prediction method may also have impacted the reported out-of-sample prediction performance.
695 Other analytical methods, such as machine learning based prediction methods, could potentially
696 yield different estimates of the behavioral prediction performance of FC measures. We also
697 acknowledge that there were differing numbers of frames across modalities. However, we
698 included this as a covariate in our analysis, which would eliminate any linear effects of the
699 number of frames on the prediction performance of each modality. Although our results were

700 similar with both 10-fold and leave-one-site-out cross validation, we acknowledge that cross-
701 validation with an independent study would be a fruitful endeavor, especially as more large-scale
702 population datasets are collected and made available to the scientific community. Finally, other
703 behavioral outcomes could be considered in the future, for instance through extraction of more
704 nuanced measures from the SST beyond reaction times, such as using drift diffusion modeling, as
705 well as modeling meaningful behaviors from the MID task that could be compared between
706 individuals.

707 **5. Conclusion**

708
709 In summary, by comparing the behavioral prediction performance of FC measures
710 derived from task fMRI to that from rsFC, we provide additional evidence that fMRI tasks that
711 evoke neural processes relevant to the behavioral phenotypes of interest are better predictors of
712 those phenotypes than FC measures from resting-state fMRI. To maximize the ability to detect
713 behaviorally relevant FC patterns of the brain, efforts should be made to select fMRI tasks that
714 recruit similar cognitive processes relevant to the behavioral phenotypes of interest. This work
715 provides further support for the utility of the task activation and FC analysis frameworks for the
716 identification of functionally relevant brain signals. It also highlights the need for consistent
717 reporting of the results of behavioral prediction studies to examine the impact of
718 sociodemographic covariates on the prediction, and to describe more clearly the prediction
719 context to which the models could be expected to generalize, based on these covariates.

720 **Acknowledgment**

721
722 The ABCD Study is a multisite, longitudinal study designed to recruit more than 10,000
723 children aged 9-10 and follow them over 10 years into early adulthood. It is supported by the
724 National Institutes of Health and additional federal partners under award numbers
725 U01DA041022, U01DA041028, U01DA041048, U01DA041089, U01DA041106,
726 U01DA041117, U01DA041120, U01DA041134, U01DA041148, U01DA041156,
727 U01DA041174, U24DA041123, U24DA041147, U01DA041093, and U01DA041025. A full list
728 of supporters is available at <https://abcdstudy.org/federal-partners.html>. A listing of participating
729 sites and a complete listing of the study investigators can be found at
730 https://abcdstudy.org/Consortium_Members.pdf. ABCD consortium investigators designed and
731 implemented the study and/or provided data but did not all necessarily participate in analysis or
732 writing of this report. This manuscript reflects the views of the authors and may not reflect the
733 opinions or views of the NIH or ABCD consortium investigators. The ABCD data repository
734 grows and changes over time.

735 **Disclosure of competing interests**

736 Dr. Dale reports that he was a Founder of and holds equity in Cor-Techs Labs, Inc., and
737 serves on its Scientific Advisory Board. He is a member of the Scientific Advisory Board of
738 Human Longevity, Inc. He receives funding through research grants from GE Healthcare to
739 UCSD. The terms of these arrangements have been reviewed by and approved by UCSD in
740 accordance with its conflict-of-interest policies. Dr. Dale also reports that he has memberships
741 with the following research consortia: Alzheimers Disease Genetics Consortium (ADGC);
742 Enhancing NeuroImaging Genetics Through Meta-analysis (ENIGMA); Prostate Cancer

- 743 Association Group to Investigate Cancer Associated Alterations in the Genome (PRACTICAL);
- 744 Psychiatric Genomics Consortium (PGC). All other authors have no conflicts of interest.

745

Reference

- 746 1. Al-Aidroos, N., Said, C.P., Turk-Browne, N.B., 2012. Top-down attention switches coupling
747 between low-level and high-level areas of human visual cortex. *Proc. Natl. Acad. Sci. U. S.*
748 *A.* 109, 14675–14680.
- 749 2. Bradley, R.H., Corwyn, R.F., 2002. Socioeconomic status and child development. *Annu.*
750 *Rev. Psychol.* 53, 371–399.
- 751 3. Brown, M.R.G., Sidhu, G.S., Greiner, R., Asgarian, N., Bastani, M., Silverstone, P.H.,
752 Greenshaw, A.J., Dursun, S.M., 2012. ADHD-200 Global Competition: diagnosing ADHD
753 using personal characteristic data can outperform resting state fMRI measurements. *Front.*
754 *Syst. Neurosci.* 6, 69.
- 755 4. Casey, B.J., Cannonier, T., Conley, M.I., Cohen, A.O., Barch, D.M., Heitzeg, M.M., Soules,
756 M.E., Teslovich, T., Dellarco, D.V., Garavan, H., Orr, C.A., Wager, T.D., Banich, M.T.,
757 Speer, N.K., Sutherland, M.T., Riedel, M.C., Dick, A.S., Bjork, J.M., Thomas, K.M.,
758 Charani, B., Mejia, M.H., Hagler, D.J., Jr, Daniela Cornejo, M., Sicat, C.S., Harms, M.P.,
759 Dosenbach, N.U.F., Rosenberg, M., Earl, E., Bartsch, H., Watts, R., Polimeni, J.R.,
760 Kuperman, J.M., Fair, D.A., Dale, A.M., ABCD Imaging Acquisition Workgroup, 2018. The
761 Adolescent Brain Cognitive Development (ABCD) study: Imaging acquisition across 21
762 sites. *Dev. Cogn. Neurosci.* 32, 43–54.
- 763 5. Castellanos, F.X., Sonuga-Barke, E.J.S., Milham, M.P., Tannock, R., 2006. Characterizing
764 cognition in ADHD: beyond executive dysfunction. *Trends Cogn. Sci.* 10, 117–123.
- 765 6. Charani, B., Hahn, S., Allgaier, N., Adise, S., Owens, M.M., Juliano, A.C., Yuan, D.K.,
766 Loso, H., Ivanciu, A., Albaugh, M.D., Dumas, J., Mackey, S., Laurent, J., Ivanova, M.,
767 Hagler, D.J., Cornejo, M.D., Hatton, S., Agrawal, A., Aguinaldo, L., Ahonen, L., Aklin, W.,

79

80

768 Anokhin, A.P., Arroyo, J., Avenevoli, S., Babcock, D., Bagot, K., Baker, F.C., Banich, M.T.,
769 Barch, D.M., Bartsch, H., Baskin-Sommers, A., Bjork, J.M., Blachman-Demner, D., Bloch,
770 M., Bogdan, R., Bookheimer, S.Y., Breslin, F., Brown, S., Calabro, F.J., Calhoun, V., Casey,
771 B.J., Chang, L., Clark, D.B., Cloak, C., Constable, R.T., Constable, K., Corley, R., Cottler,
772 L.B., Coxe, S., Dagher, R.K., Dale, A.M., Dapretto, M., Delcarmen-Wiggins, R., Dick, A.S.,
773 Do, E.K., Dosenbach, N.U.F., Dowling, G.J., Edwards, S., Ernst, T.M., Fair, D.A., Fan, C.C.,
774 Feczko, E., Feldstein-Ewing, S.W., Florsheim, P., Foxe, J.J., Freedman, E.G., Friedman,
775 N.P., Friedman-Hill, S., Fuemmeler, B.F., Galvan, A., Gee, D.G., Giedd, J., Glantz, M.,
776 Glaser, P., Godino, J., Gonzalez, M., Gonzalez, R., Grant, S., Gray, K.M., Haist, F., Harms,
777 M.P., Hawes, S., Heath, A.C., Heeringa, S., Heitzeg, M.M., Hermosillo, R., Herting, M.M.,
778 Hettema, J.M., Hewitt, J.K., Heyser, C., Hoffman, E., Howlett, K., Huber, R.S., Huestis,
779 M.A., Hyde, L.W., Iacono, W.G., Infante, M.A., Irfanoglu, O., Isaiah, A., Iyengar, S.,
780 Jacobus, J., James, R., Jean-Francois, B., Jernigan, T., Karcher, N.R., Kaufman, A., Kelley,
781 B., Kit, B., Ksinan, A., Kuperman, J., Laird, A.R., Larson, C., LeBlanc, K., Lessov-
782 Schlagger, C., Lever, N., Lewis, D.A., Lisdahl, K., Little, A.R., Lopez, M., Luciana, M.,
783 Luna, B., Madden, P.A., Maes, H.H., Makowski, C., Marshall, A.T., Mason, M.J., Matochik,
784 J., McCandliss, B.D., McGlade, E., Montoya, I., Morgan, G., Morris, A., Mulford, C.,
785 Murray, P., Nagel, B.J., Neale, M.C., Neigh, G., Nencka, A., Noronha, A., Nixon, S.J.,
786 Palmer, C.E., Pariyadath, V., Paulus, M.P., Pelham, W.E., Pfefferbaum, D., Pierpaoli, C.,
787 Prescott, A., Prouty, D., Puttler, L.I., Rajapaske, N., Rapuano, K.M., Reeves, G., Renshaw,
788 P.F., Riedel, M.C., Rojas, P., de la Rosa, M., Rosenberg, M.D., Ross, M.J., Sanchez, M.,
789 Schirda, C., Schloesser, D., Schulenberg, J., Sher, K.J., Sheth, C., Shilling, P.D., Simmons,
790 W.K., Sowell, E.R., Speer, N., Spittel, M., Squeglia, L.M., Sripada, C., Steinberg, J., Striley,

- 791 C., Sutherland, M.T., Tanabe, J., Tapert, S.F., Thompson, W., Tomko, R.L., Uban, K.A.,
792 Vrieze, S., Wade, N.E., Watts, R., Weiss, S., Wiens, B.A., Williams, O.D., Wilbur, A., Wing,
793 D., Wolff-Hughes, D., Yang, R., Yurgelun-Todd, D.A., Zucker, R.A., Potter, A., Garavan,
794 H.P., ABCD Consortium, 2021. Baseline brain function in the preadolescents of the ABCD
795 Study. *Nat. Neurosci.* 24, 1176–1186.
- 796 7. Challis, E., Hurley, P., Serra, L., Bozzali, M., Oliver, S., Cercignani, M., 2015. Gaussian
797 process classification of Alzheimer’s disease and mild cognitive impairment from resting-
798 state fMRI. *Neuroimage* 112, 232–243.
- 799 8. Chen, J., Tam, A., Kebets, V., Orban, C., Ooi, L.Q.R., Asplund, C.L., Marek, S., Dosenbach,
800 N.U.F., Eickhoff, S.B., Bzdok, D., Holmes, A.J., Yeo, B.T.T., 2022. Shared and unique brain
801 network features predict cognitive, personality, and mental health scores in the ABCD study.
802 *Nat. Commun.* 13, 2217.
- 803 9. Cole, M.W., Bassett, D.S., Power, J.D., Braver, T.S., Petersen, S.E., 2014. Intrinsic and task-
804 evoked network architectures of the human brain. *Neuron* 83, 238–251.
- 805 10. Cole, M.W., Ito, T., Cocuzza, C., Sanchez-Romero, R., 2021. The Functional Relevance of
806 Task-State Functional Connectivity. *J. Neurosci.* 41, 2684–2702.
- 807 11. Dosenbach, N.U.F., Nardos, B., Cohen, A.L., Fair, D.A., Power, J.D., Church, J.A., Nelson,
808 S.M., Wig, G.S., Vogel, A.C., Lessov-Schlaggar, C.N., Barnes, K.A., Dubis, J.W., Feczko,
809 E., Coalson, R.S., Pruett, J.R., Jr., Barch, D.M., Petersen, S.E., Schlaggar, B.L., 2010.
810 Prediction of Individual Brain Maturity Using fMRI. *Science* 329.
- 811 12. Elliott, M.L., Knodt, A.R., Cooke, M., Kim, M.J., Melzer, T.R., Keenan, R., Ireland, D.,
812 Ramrakha, S., Poulton, R., Caspi, A., Moffitt, T.E., Hariri, A.R., 2019. General functional

813 connectivity: Shared features of resting-state and task fMRI drive reliable and heritable
814 individual differences in functional brain networks. *Neuroimage* 189, 516–532.

815 13. Fair, D.A., Miranda-Dominguez, O., Snyder, A.Z., Perrone, A., Earl, E.A., Van, A.N.,
816 Koller, J.M., Feczko, E., Klein, R.L., Mirro, A.E., Hampton, J.M., Adeyemo, B., Laumann,
817 T.O., Gratton, C., Greene, D.J., Schlaggar, B.L., Hagler, D., Watts, R., Garavan, H., Barch,
818 D.M., Nigg, J.T., Petersen, S.E., Dale, A., Feldstein-Ewing, S.W., Nagel, B.J., Dosenbach,
819 N.U.F., 2018. Correction of respiratory artifacts in MRI head motion estimates. *bioRxiv*.

820 14. Fair, D.A., Schlaggar, B.L., Cohen, A.L., Miezin, F.M., Dosenbach, N.U.F., Wenger, K.K.,
821 Fox, M.D., Snyder, A.Z., Raichle, M.E., Petersen, S.E., 2007. A method for using blocked
822 and event-related fMRI data to study “resting state” functional connectivity. *Neuroimage* 35,
823 396–405.

824 15. Fan, C.C., Palmer, C.E., Iverson, J., Pecheva, D., Thompson, W.K., Hagler, D., Jernigan,
825 T.L., Dale, A.M., 2021. FEMA: Fast and efficient mixed-effects algorithm for population-
826 scale whole brain imaging data. *bioRxiv*.

827 16. Farah, M.J., 2018. Socioeconomic status and the brain: prospects for neuroscience-informed
828 policy. *Nat. Rev. Neurosci.* 19, 428–438.

829 17. Finn, E.S., Bandettini, P.A., 2021. Movie-watching outperforms rest for functional
830 connectivity-based prediction of behavior. *Neuroimage* 235, 117963.

831 18. Finn, E.S., Scheinost, D., Finn, D.M., Shen, X., Papademetris, X., Constable, R.T., 2017.
832 Can brain state be manipulated to emphasize individual differences in functional
833 connectivity? *Neuroimage* 160, 140–151.

- 834 19. Finn, E.S., Shen, X., Scheinost, D., Rosenberg, M.D., Huang, J., Chun, M.M., Papademetris,
835 X., Constable, R.T., 2015. Functional connectome fingerprinting: identifying individuals
836 using patterns of brain connectivity. *Nat. Neurosci.* 18, 1664–1671.
- 837 20. Fischl, B., Salat, D.H., Busa, E., Albert, M., Dieterich, M., Haselgrove, C., van der Kouwe,
838 A., Killiany, R., Kennedy, D., Klaveness, S., Montillo, A., Makris, N., Rosen, B., Dale,
839 A.M., 2002. Whole Brain Segmentation: Neurotechnique Automated Labeling of
840 Neuroanatomical Structures in the Human Brain. *Neuron* 33, 341–355.
- 841 21. Gabrieli, J.D.E., Ghosh, S.S., Whitfield-Gabrieli, S., 2015. Prediction as a humanitarian and
842 pragmatic contribution from human cognitive neuroscience. *Neuron* 85, 11–26.
- 843 22. Gao, S., Greene, A.S., Constable, R.T., Scheinost, D., 2019. Combining multiple
844 connectomes improves predictive modeling of phenotypic measures. *Neuroimage* 201,
845 116038.
- 846 23. Garavan, H., Bartsch, H., Conway, K., Decastro, A., Goldstein, R.Z., Heeringa, S., Jernigan,
847 T., Potter, A., Thompson, W., Zahs, D., 2018. Recruiting the ABCD sample: Design
848 considerations and procedures. *Dev. Cogn. Neurosci.* 32, 16–22.
- 849 24. Gauggel, S., Rieger, M., Feghoff, T.-A., 2004. Inhibition of ongoing responses in patients
850 with Parkinson’s disease. *J. Neurol. Neurosurg. Psychiatry* 75, 539–544.
- 851 25. Gordon, E.M., Laumann, T.O., Adeyemo, B., Huckins, J.F., Kelley, W.M., Petersen, S.E.,
852 2016. Generation and Evaluation of a Cortical Area Parcellation from Resting-State
853 Correlations. *Cereb. Cortex* 26, 288–303.
- 854 26. Gratton, C., Laumann, T.O., Nielsen, A.N., Greene, D.J., Gordon, E.M., Gilmore, A.W.,
855 Nelson, S.M., Coalson, R.S., Snyder, A.Z., Schlaggar, B.L., Dosenbach, N.U.F., Petersen,

856 S.E., 2018. Functional Brain Networks Are Dominated by Stable Group and Individual
857 Factors, Not Cognitive or Daily Variation. *Neuron* 98, 439–452.e5.

858 27. Greene, A.S., Gao, S., Noble, S., Scheinost, D., Constable, R.T., 2020. How Tasks Change
859 Whole-Brain Functional Organization to Reveal Brain-Phenotype Relationships. *Cell Rep.*
860 32, 108066.

861 28. Greene, A.S., Gao, S., Scheinost, D., Constable, R.T., 2018. Task-induced brain state
862 manipulation improves prediction of individual traits. *Nat. Commun.* 9, 2807.

863 29. Hagler, D.J., Hatton, S.N., Makowski, C., Daniela Cornejo, M., Fair, D.A., Dick, A.S.,
864 Sutherland, M.T., Casey, B.J., Barch, D.M., Harms, M.P., Watts, R., Bjork, J.M., Garavan,
865 H.P., Hilmer, L., Pung, C.J., Sicat, C.S., Kuperman, J., Bartsch, H., Xue, F., Heitzeg, M.M.,
866 Laird, A.R., Trinh, T.T., Gonzalez, R., Tapert, S.F., Riedel, M.C., Squeglia, L.M., Hyde,
867 L.W., Rosenberg, M.D., Earl, E.A., Howlett, K.D., Baker, F.C., Soules, M., Diaz, J., de
868 Leon, O.R., Thompson, W.K., Neale, M.C., Herting, M., Sowell, E.R., Alvarez, R.P., Hawes,
869 S.W., Sanchez, M., Bodurka, J., Breslin, F.J., Morris, A.S., Paulus, M.P., Kyle Simmons, W.,
870 Polimeni, J.R., van der Kouwe, A., Nencka, A.S., Gray, K.M., Pierpaoli, C., Matochik, J.A.,
871 Noronha, A., Aklin, W.M., Conway, K., Glantz, M., Hoffman, E., Little, R., Lopez, M.,
872 Pariyadath, V., Weiss, S.R.B., Wolff-Hughes, D.L., DelCarmen-Wiggins, R., Feldstein
873 Ewing, S.W., Miranda-Dominguez, O., Nagel, B.J., Perrone, A.J., Sturgeon, D.T., Goldstone,
874 A., Pfefferbaum, A., Pohl, K.M., Prouty, D., Uban, K., Bookheimer, S.Y., Dapretto, M.,
875 Galvan, A., Bagot, K., Giedd, J., Alejandra Infante, M., Jacobus, J., Patrick, K., Shilling,
876 P.D., Desikan, R., Li, Y., Sugrue, L., Banich, M.T., Friedman, N., Hewitt, J.K., Hopfer, C.,
877 Sakai, J., Tanabe, J., Cottler, L.B., Nixon, S.J., Chang, L., Cloak, C., Ernst, T., Reeves, G.,
878 Kennedy, D.N., Heeringa, S., Peltier, S., Schulenberg, J., Sripada, C., Zucker, R.A., Iacono,

879 W.G., Luciana, M., Calabro, F.J., Clark, D.B., Lewis, D.A., Luna, B., Schirda, C., Brima, T.,
880 Foxe, J.J., Freedman, E.G., Mruzek, D.W., Mason, M.J., Huber, R., McGlade, E., Prescott,
881 A., Renshaw, P.F., Yurgelun-Todd, D.A., Allgaier, N.A., Dumas, J.A., Ivanova, M., Potter,
882 A., Florsheim, P., Larson, C., Lisdahl, K., Charness, M.E., Fuemmeler, B., Hetteima, J.M.,
883 Steinberg, J., Anokhin, A.P., Glaser, P., Heath, A.C., Madden, P.A., Baskin-Sommers, A.,
884 Todd Constable, R., Grant, S.J., Dowling, G.J., Brown, S.A., Jernigan, T.L., Dale, A.M.,
885 2018. Image processing and analysis methods for the Adolescent Brain Cognitive
886 Development Study. bioRxiv.

887 30. Hallquist, M.N., Hwang, K., Luna, B., 2013. The nuisance of nuisance regression: spectral
888 misspecification in a common approach to resting-state fMRI preprocessing reintroduces
889 noise and obscures functional connectivity. *Neuroimage* 82, 208–225.

890 31. Hyatt, C.S., Owens, M.M., Crowe, M.L., Carter, N.T., Lynam, D.R., Miller, J.D., 2020. The
891 quandary of covarying: A brief review and empirical examination of covariate use in
892 structural neuroimaging studies on psychological variables. *Neuroimage* 205, 116225.

893 32. Jurkiewicz, M.T., Crawley, A.P., Mikulis, D.J., 2018. Is Rest Really Rest? Resting-State
894 Functional Connectivity During Rest and Motor Task Paradigms. *Brain Connect.* 8, 268–275.

895 33. Kardan, O., Stier, A.J., Cardenas-Iniguez, C., Schertz, K.E., Pruin, J.C., Deng, Y.,
896 Chamberlain, T., Meredith, W.J., Zhang, X., Bowman, J.E., Lakhtakia, T., Tindel, L., Avery,
897 E.W., Lin, Q., Yoo, K., Chun, M.M., Berman, M.G., Rosenberg, M.D., 2022. Differences in
898 the functional brain architecture of sustained attention and working memory in youth and
899 adults. *PLoS Biol.* 20, e3001938.

900

- 901 34. Khazaei, A., Ebrahimzadeh, A., Babajani-Feremi, A., 2016. Application of advanced
902 machine learning methods on resting-state fMRI network for identification of mild cognitive
903 impairment and Alzheimer's disease. *Brain Imaging Behav.* 10, 799–817.
- 904 35. Kim, J., Calhoun, V.D., Shim, E., Lee, J.-H., 2016. Deep neural network with weight sparsity
905 control and pre-training extracts hierarchical features and enhances classification
906 performance: Evidence from whole-brain resting-state functional connectivity patterns of
907 schizophrenia. *Neuroimage* 124, 127–146.
- 908 36. Korous, K.M., Causadias, J.M., Bradley, R.H., Luthar, S.S., Levy, R., 2020. A Systematic
909 Overview of Meta-Analyses on Socioeconomic Status, Cognitive Ability, and Achievement:
910 The Need to Focus on Specific Pathways. *Psychol. Rep.* 33294120984127.
- 911 37. Kowalski, J., Wypych, M., Marchewka, A., Dragan, M., 2019. Neural Correlates of
912 Cognitive-Attentional Syndrome: An fMRI Study on Repetitive Negative Thinking Induction
913 and Resting State Functional Connectivity. *Front. Psychol.* 10, 648.
- 914 38. Larabi, D.I., van der Meer, L., Pijnenborg, G.H.M., Ćurčić-Blake, B., Aleman, A., 2018.
915 Insight and emotion regulation in schizophrenia: A brain activation and functional
916 connectivity study. *Neuroimage Clin* 20, 762–771.
- 917 39. Laumann, T.O., Gordon, E.M., Adeyemo, B., Snyder, A.Z., Joo, S.J., Chen, M.-Y., Gilmore,
918 A.W., McDermott, K.B., Nelson, S.M., Dosenbach, N.U.F., Schlaggar, B.L., Mumford, J.A.,
919 Poldrack, R.A., Petersen, S.E., 2015. Functional System and Areal Organization of a Highly
920 Sampled Individual Human Brain. *Neuron* 87, 657–670.
- 921 40. Liu, Z., Zhang, Y., Yan, H., Bai, L., Dai, R., Wei, W., Zhong, C., Xue, T., Wang, H., Feng,
922 Y., You, Y., Zhang, X., Tian, J., 2012. Altered topological patterns of brain networks in mild

- 923 cognitive impairment and Alzheimer's disease: a resting-state fMRI study. *Psychiatry Res.*
924 202, 118–125.
- 925 41. Luciana, M., Bjork, J.M., Nagel, B.J., Barch, D.M., Gonzalez, R., Nixon, S.J., Banich, M.T.,
926 2018. Adolescent neurocognitive development and impacts of substance use: Overview of
927 the adolescent brain cognitive development (ABCD) baseline neurocognition battery. *Dev.*
928 *Cogn. Neurosci.* 32, 67–79.
- 929 42. Lynam, D.R., Hoyle, R.H., Newman, J.P., 2006. The perils of partialling: cautionary tales
930 from aggression and psychopathy. *Assessment* 13, 328–341.
- 931 43. Moutoussis, M., Garzón, B., Neufeld, S., Bach, D.R., Rigoli, F., Goodyer, I., Bullmore, E.,
932 NSPN Consortium, Guitart-Masip, M., Dolan, R.J., 2021. Decision-making ability,
933 psychopathology, and brain connectivity. *Neuron* 109, 2025–2040.e7.
- 934 44. Nielsen, A.N., Greene, D.J., Gratton, C., Dosenbach, N.U.F., Petersen, S.E., Schlaggar, B.L.,
935 2019. Evaluating the Prediction of Brain Maturity From Functional Connectivity After
936 Motion Artifact Denoising. *Cereb. Cortex* 29, 2455–2469.
- 937 45. Palmer, C.E., Zhao, W., Loughnan, R., Zou, J., Fan, C.C., Thompson, W.K., Dale, A.M.,
938 Jernigan, T.L., 2021. Distinct Regionalization Patterns of Cortical Morphology are
939 Associated with Cognitive Performance Across Different Domains. *Cereb. Cortex* 31, 3856–
940 3871.
- 941 46. Power, J.D., Mitra, A., Laumann, T.O., Snyder, A.Z., Schlaggar, B.L., Petersen, S.E., 2014.
942 Methods to detect, characterize, and remove motion artifact in resting state fMRI.
943 *Neuroimage* 84, 320–341.
- 944 47. Qian, X., Loo, B.R.Y., Castellanos, F.X., Liu, S., Koh, H.L., Poh, X.W.W., Krishnan, R.,
945 Fung, D., Chee, M.W., Guan, C., Lee, T.-S., Lim, C.G., Zhou, J., 2018. Brain-computer-

946 interface-based intervention re-normalizes brain functional network topology in children with
947 attention deficit/hyperactivity disorder. *Transl. Psychiatry* 8, 149.

948 48. Rakesh, D., Zalesky, A., Whittle, S., 2021. Similar but distinct - Effects of different
949 socioeconomic indicators on resting state functional connectivity: Findings from the
950 Adolescent Brain Cognitive Development (ABCD) Study®. *Dev. Cogn. Neurosci.* 51,
951 101005.

952 49. Rosenberg, M.D., Finn, E.S., Scheinost, D., Papademetris, X., Shen, X., Constable, R.T.,
953 Chun, M.M., 2016. A neuromarker of sustained attention from whole-brain functional
954 connectivity. *Nat. Neurosci.* 19, 165–171.

955 50. Satterthwaite, T.D., Wolf, D.H., Loughead, J., Ruparel, K., Elliott, M.A., Hakonarson, H.,
956 Gur, R.C., Gur, R.E., 2012. Impact of in-scanner head motion on multiple measures of
957 functional connectivity: relevance for studies of neurodevelopment in youth. *Neuroimage* 60,
958 623–632.

959 51. Simmons, J.P., Nelson, L.D., Simonsohn, U., 2011. False-positive psychology: undisclosed
960 flexibility in data collection and analysis allows presenting anything as significant. *Psychol.*
961 *Sci.* 22, 1359–1366.

962 52. Speer, S.P.H., Smidts, A., Boksem, M.A.S., 2021. Individual differences in (dis)honesty are
963 represented in the brain’s functional connectivity at rest. *Neuroimage* 246, 118761.

964 53. Sripada, C., Angstadt, M., Taxali, A., Clark, D.A., Greathouse, T., Rutherford, S., Dickens,
965 J.R., Shedden, K., Gard, A.M., Hyde, L.W., Weigard, A., Heitzeg, M., 2021. Brain-wide
966 functional connectivity patterns support general cognitive ability and mediate effects of
967 socioeconomic status in youth. *Transl. Psychiatry* 11, 571.

- 968 54. Sripada, C., Rutherford, S., Angstadt, M., Thompson, W.K., Luciana, M., Weigard, A.,
969 Hyde, L.H., Heitzeg, M., 2019. Prediction of neurocognition in youth from resting state
970 fMRI. *Mol. Psychiatry*.
- 971 55. Taylor, R.L., Cooper, S.R., Jackson, J.J., Barch, D.M., 2020. Assessment of Neighborhood
972 Poverty, Cognitive Function, and Prefrontal and Hippocampal Volumes in Children. *JAMA*
973 *Netw Open* 3, e2023774.
- 974 56. Thomas, R.M., Gallo, S., Cerliani, L., Zhutovsky, P., El-Gazzar, A., van Wingen, G., 2020.
975 Classifying Autism Spectrum Disorder Using the Temporal Statistics of Resting-State
976 Functional MRI Data With 3D Convolutional Neural Networks. *Front. Psychiatry* 11, 440.
- 977 57. Vanderwal, T., Eilbott, J., Finn, E.S., Craddock, R.C., Turnbull, A., Castellanos, F.X., 2017.
978 Individual differences in functional connectivity during naturalistic viewing conditions.
979 *Neuroimage* 157, 521–530.
- 980 58. Varoquaux, G., Poldrack, R.A., 2019. Predictive models avoid excessive reductionism in
981 cognitive neuroimaging. *Curr. Opin. Neurobiol.* 55, 1–6.
- 982 59. Wagenmakers, E.-J., Sarafoglou, A., Aczel, B., 2022. One statistical analysis must not rule
983 them all [WWW Document]. Nature Publishing Group UK. URL
984 <http://dx.doi.org/10.1038/d41586-022-01332-8> (accessed 8.10.22).
- 985 60. Yaple, Z.A., Yu, R., 2020. Functional and Structural Brain Correlates of Socioeconomic
986 Status. *Cereb. Cortex* 30, 181–196.
- 987 61. Zhang, M., Nathaniel, U., Savill, N., Smallwood, J., Jefferies, E., 2021. Intrinsic connectivity
988 of left ventrolateral prefrontal cortex predicts individual differences in controlled semantic
989 retrieval. *Neuroimage* 246, 118760.

990 62. Zhao, W., Palmer, C.E., Thompson, W.K., Charani, B., Garavan, H.P., Casey, B.J.,
991 Jernigan, T.L., Dale, A.M., Fan, C.C., 2021. Individual Differences in Cognitive Performance
992 Are Better Predicted by Global Rather Than Localized BOLD Activity Patterns Across the
993 Cortex. *Cereb. Cortex* 31, 1478–1488.